Available online at www.sciencedirect.com
ScienceDirect
Cement and Concrete Research 37 (2007) 469–480
Cement and Concrete Research

Modeling of the link between microstructure and effective diffusivity of cement pastes using a simplified composite model

S. Bejaoui *, B. Bary [1]

CEA Saclay, DEN/DPC/SCCME/LECBA, 91191 Gif/Yvette, France

Received 24 October 2005; accepted 19 June 2006

Abstract

The knowledge of the relationship between porosity and transport properties of concrete is a point of major importance to run properly the models coupling chemistry, transport and mechanics in order to simulate the engineered barrier degradations in the context of the nuclear waste deep repository. The present work proposes a simplified composite model aiming at linking microstructure and effective diffusivity of cement pastes. The proposed analytical method allows the estimation of the evolution of effective diffusivity of such materials submitted to porosity opening or plugging, at the scale of the Representative Elementary Volume (REV). The method is then applied to Ordinary Portland Cement (OPC) pastes. The porosity–diffusion evolutions determined from the composite model for various OPC pastes are implemented into simplified chemo-transport simulations aiming at describing the leaching of cementitious materials. Using these evolutions, OPC paste leaching simulations are in good agreement with the available experimental data, indicating a good reliability of the simplified composite model.

Keywords: Microstructure; Diffusion; Composite model; Cement paste; Durability

1. Introduction

In the various nuclear waste deep repository concepts, concrete will be subjected in the long term to solicitations by underground water and will undergo degradations depending on the various ions present in the aggressive solution [1]. Due to leaching, carbonation, sulfate attack, etc., mechanical and confinement properties of concrete may consequently (progressively) evolve. In this context, the degradations of concrete engineered barrier are generally predicted on the basis of experiments and using models coupling chemistry, transport and mechanics [2–5]. These tools require in particular the knowledge of the local evolution of the transport properties of concrete according to the modifications of their porosity induced by the degradations. Indeed, these latter can induce porosity opening or plugging, and possibly cracking, due to the dissolution or the precipitation of minerals in the system. These phenomena may generate in turn significant modifications of the local transport properties which need to be quantified in order to properly simulate the concrete long term behavior.

The link between porosity (or microstructure) and transport properties of cementitious materials is investigated hereafter. More precisely, this study deals with the diffusion of the chemical species present in the pore water of cement pastes submitted to porosity changes. The material will be considered fully saturated, with a constant pore pressure (consequently no convective transport is possible). The impacts of cracking and aggregates on the diffusivity of cementitious materials have been studied elsewhere [6–11] and are not investigated here. Neither are electro-diffusion effects that can be taken into account specifically using the appropriated Nernst–Planck transport formulation (see e.g. [12]).

Because of the complex and multi-scale porosity of cement pastes, empirical porosity–diffusion evolutions are generally used in most contributions [6,13,14]. The drawbacks of using empirical laws lie in the fact that the basic phenomena remain poorly understood. Using deterministic modeling should contribute to reach a better understanding of the phenomenology and thus to improve the reliability of concrete long term behavior simulations. Composite and homogenization methods seem well

* Corresponding author. Tel.: +33 1 69 08 23 83; fax: +33 1 69 08 84 41.
E-mail address: syriac.bejaoui@cea.fr (S. Bejaoui).
[1] Tel.: +33 4 42 25 33 07; fax: +33 4 42 25 70 42.

0008-8846/$ - see front matter © 2006 Elsevier Ltd. All rights reserved.
doi:10.1016/j.cemconres.2006.06.004

adapted to treat the problem. Their goal is to calculate the property of an heterogeneous system at the scale of the Representative Elementary Volume (REV) considering the elementary properties of the components of the system and its microstructure (see e.g. [15]). A three-dimensional numerical method was developed to achieve this goal [16]. Using the numerical description of hydrated OPC pastes obtained with the CEMHYD3D three-dimensional hydration code [17], the tool allows to calculate the effective diffusivity (for a given specie) of the system as a function of the self-diffusion coefficients of capillary porosity and calcium silicate hydrates (C–S–H) by converting the 3D digital image into a random conductor network [18]. The self-diffusion coefficient of C–S–H was identified on the basis of macroscopic diffusion experimental results by using of inverse analysis. The diffusivities of a number of OPC pastes were then calculated using this tool, and a modified Archie law linking the capillary porosity and the relative effective diffusivity of OPC pastes was fitted on the results [16]. The authors have found that the percolation threshold of capillary porosity is about 0.17 using their three-dimensional hydration code. For systems in which the amount of capillary porosity is lower *(higher)* than this value, the diffusion flow is principally controlled by the C–S–H porous matrix *(capillary porosity)*. Parameters are used to adjust the coefficients of the modified Archie law to account for the impact of silica fume addition on the self-diffusion coefficient of C–S–H. Another contribution proposes to deal with the problem by using the general effective media equation [19]. The diffusion through capillary porosity and C–S–H is considered and the formulation allows accounting for a geometrical percolation threshold of capillary porosity. However, these modeling methods do not describe precisely the composition of the C–S–H matrix. Thus, its self-diffusion coefficient changes for example with the addition of silica fume [16,19] and the type of cement [19] according to empirical evolutions. In order to get a more precise description of the C–S–H matrix in the case of OPC pastes, the C–S–H can be described according to the Jennings model which consider two types of this hydrate: the Low Density and the High Density C–S–H [20,21]. These two types of C–S–H and the capillary porosity are taken into account in a homogenization model aiming at estimating the diffusivity of OPC pastes submitted to porosity opening (leaching) and plugging (carbonation) [22]. The method is based on a multi-coated sphere assemblage formulation that provides exact solutions.

This paper presents a simplified composite model, namely Microtrans, which avoids the problem of the multi-scale porosity description by only considering the system at the micro scale. At this scale, the phases contributing to transport in OPC pastes are the capillary porosity and the Low Density and High density C–S–H. As defined elsewhere, capillary porosity is supposed to consist of pores larger than about 0.1 μm (see e.g. [23]). Nanoporosity (pore sizes situated between about 1 nm and a few tens of nanometers [23]) is described here as being a part of C–S–H, and is directly taken into account in the LD and HD C–S–H phases [20,21]. The percolation phenomena of the diffusive phases are explicitly taken into account in the model. The method, which presents the advantages of being simple and non-empirical, allows the estimation of the effective diffusion coefficient of OPC pastes submitted to porosity opening and plugging at the REV scale. The formalism of the model and its application to the case of OPC pastes are presented in the first part of this paper. Second, the porosity–diffusion evolutions estimated by the composite tool for various OPC pastes are implemented into a simplified chemo-transport model aiming at describing the leaching of cementitious materials. Using these evolutions, OPC paste leaching simulations are in good agreement with the available experimental data in terms of degradation depths and leached zone diffusivities, indicating a good reliability of the simplified composite model.

2. Description of the Microtrans model

2.1. Experimental data

The model is build up on experimental data stemming from diffusion experiments carried out on hardened cement pastes mixed with an ordinary portland cement (OPC). Data related to pastes mixed with a blended cement with blast furnace slag and pulverized fly ash (BFS-PFA cement) are also given for comparison. However, as it will be explained later in Section 2.3, no modeling work is carried out for BFS-PFA materials in this paper. Characteristics of the cements are given in Table 1. The water to cement mass ratios (w/c) were ranging from 0.25 to 0.70, in order to study materials over a large range of performances. Cylindrical samples, of 70 mm diameter and 100 mm high, were cured in saturated lime water incorporating sodium and potassium hydroxide, during 12 months for OPC pastes and 18 months for BFS-PFA cement pastes. Then, samples were cut to obtain 4-mm-thick discs in order to perform tritiated water (HTO) diffusion tests.

Diffusion experiments were carried out in diffusion cells, containing an upstream compartment filled with water in equilibrium with portlandite and doped with HTO, and a downstream compartment filled with the same type of inactive liquid. The two cells were separated by a sample of the material to characterize. Due to a concentration unbalance between compartments, diffusion takes place. The downstream

Table 1
Characteristics of OPC and BFS-PFA cements

Components (mass %)	OPC	BFS-PFA cement
Clinker	100	51
Slag	–	25
Fly ash	–	24
Gypsum added	7	4
Chemical composition (mass %)		
SiO_2	23.7	29.0
Al_2O_3	2.8	10.8
Fe_2O_3	2.3	3.3
CaO	67.3	45.5
MgO	0.7	2.5
SO_3	1.9	2.6
K_2O+Na_2O	0.2	1.5
Density (g/cm^3)	3.2	2.9
Specific area (cm^2/g)	3105	4700
Compressive strength at 28 days (MPa)	60	46

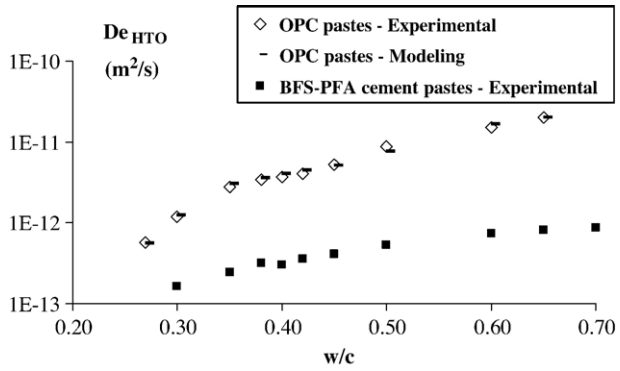

Fig. 1. Effective diffusion coefficients of tritiated water (HTO) for OPC and BFS-PFA cement pastes as a function of w/c ratio (experimental and modeling results).

compartment is emptied at predetermined times and filled by inactive solution, thus maintaining a quasi zero concentration. The diffusion is modeled using Fick's law. When the steady state is obtained, the cumulated release gives access to an effective diffusion coefficient of tritiated water (De_{HTO}) in the sample. Then, a simple program can estimate a corrected value of De_{HTO} taking into account the upstream activity balance, isotopic exchange, activity present in the sample, downstream released activities and decay. Experimental results are given in Fig. 1 (together with modeling results obtained using the simplified composite model, as presented in the next sections).

As it is shown in Fig. 1, whatever the w/c ratio, De_{HTO} of BFS-PFA cement pastes are about one order of magnitude smaller than those related to OPC pastes. However, after 4 months curing, water porosities of OPC pastes made with various w/c (0.30, 0.40 and 0.50) were found to be slightly lower than the ones of BFS-PFA cement pastes made with similar w/c (for details, see Ref. [24] in which porosity measurements were performed on the same materials as the ones used in this study). That illustrates the fact that it is not possible in general to establish a generic relationship between total porosity and diffusivity for cement-based materials. The next section presents the formalism of the Microtrans composite model aiming at linking microscopic features and effective diffusivity of heterogeneous cementitious systems.

2.2. Formalism of the model

This part is dedicated to the presentation of the general formalism of the model. The application of the model to the case of OPC pastes will be the purpose of the next section.

Let us consider an isotropic system made up of two phases having different self-diffusion coefficients (for a given diffusing species) (Fig. 2 left). The volume fraction of the matrix (phase 1) in the system is equal to Q_1 and its self-diffusion coefficient is equal to D_{sd1}. The same notations are adopted for the inclusions (phase 2) and it is considered that $D_{sd2} > D_{sd1}$. The total effective diffusivity of the composite material at the REV scale is equal to De. It is assumed that the system presented in Fig. 2 left may be approximated with good accuracy by the simplified one represented in Fig. 2 right. In this new system, the percolating fraction of the most diffusive phase (yQ_2) is placed in parallel in the assemblage, whereas the remaining fraction which does not percolate ($(1-y)Q_2$) is placed in series with the other phase. This disposition of the phases in the equivalent system allows accounting for the fact that the diffusive flow is essentially controlled by the most diffusive phase percolating in the system. For simplicity, the non-percolating fraction of the most diffusive phase is then integrated in series with the less diffusive phase to compose a mixed component. In this mixed component, the diffusive transport is controlled by the less diffusive phase (see Fig. 2 right). It may then be interpreted as a matrix in which are distributed inclusions of the most diffusive phases. This last aspect will be discussed in more details in the next section.

As stated before, the diffusive transport in the modeled system (Fig. 2 right) is assumed to occur through a first component, the percolating fraction of phase 2, and through a second one, the mixed component. However, the 3D geometrical properties (tortuosity, constrictivity) of these various percolating diffusing components (single percolating phases or mixed components) are lost when transposing the 3D system (Fig. 2 left) to the simplified 2D modeled one (Fig. 2 right). To correct this point, a tortuosity coefficient is attributed to each diffusive component (see e.g. [25]). It allows accounting for the 3D disposition of the diffusive component in the system. This approach has the advantage of conserving a simple, analytical and exact form for the diffusivity estimate in the case of parallel distribution of phases.

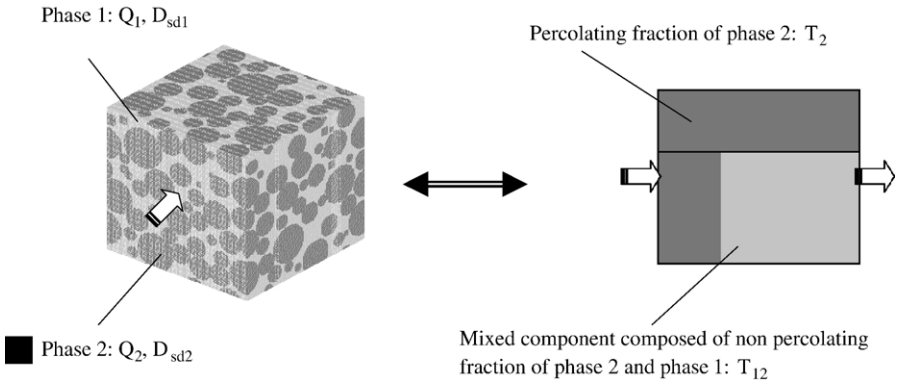

Fig. 2. Sketch of a system made up of two phases having different self-diffusion coefficients ($D_{sd2} > D_{sd1}$) (left) and its equivalent system in the Microtrans model (right). The arrows indicate the direction of the diffusing species through the system.

Indeed, if both of the two phases composing the parallel system fully percolate ($y=1$), the composite effective diffusion coefficient can be calculated using Eq. (1). In Eq. (1), De_1 and De_2 are respectively the contributions of phase 1 and 2 to the effective composite diffusivity, and $T_1(Q_1)$ and $T_2(Q_2)$ are respectively the tortuosity coefficients related to phase 1 and 2.

$$De = De_1 + De_2 = \left[Q_1 D_{sd1} \frac{1}{T_1(Q_1)}\right] + \left[Q_2 D_{sd2} \frac{1}{T_2(Q_2)}\right] \quad (1)$$

It is worth noticing that the tortuosity coefficient $T_2(Q_2)$ is directly related to the formation factor $F_2(Q_2)$ through the following definition:

$$\frac{De}{D_{sd2}} = \frac{Q_2}{T_2(Q_2)} = \frac{1}{F_2(Q_2)}. \quad (2a)$$

in the case where the material is composed of a perfectly insulating matrix and a connected diffusive phase (so as to obtain an infinite contrast) with diffusivity and volume fraction D_{sd2} and Q_2, respectively (see e.g. [25,26]). For a composite having two diffusive phases with diffusivity D_{sd1} and D_{sd2}, the above definition simply specializes into:

$$\begin{aligned} \lim_{D_{sd2}\to\infty} \frac{De}{D_{sd2}} &= \frac{Q_2}{T_2(Q_2)} = \frac{1}{F_2(Q_2)}, \\ \lim_{D_{sd1}\to\infty} \frac{De}{D_{sd1}} &= \frac{Q_1}{T_1(Q_1)} = \frac{1}{F_1(Q_1)} \end{aligned} \quad (2b)$$

Now, if only a fraction of phase 2 is percolating (as shown in Fig. 2), it is assumed that the composite effective diffusion coefficient can be estimated with good accuracy using Eq. (3), which is an extension on Eq. (1). $T_2(yQ_2)$ and $T_{12}[(1-y)Q_2+Q_1]$ in Eq. (3) are respectively the tortuosity coefficients related to the percolating fraction of phase 2, and to the mixed diffusive component composed of phase 1 and the non-percolating fraction of phase 2 (see Fig. 2 right). The form of the second term in the right-hand side of Eq. (3) follows from considering that the mixed component self-diffusivity is simply obtained by applying the series (harmonic) average to the diffusivities of its components.

$$De = \left[yQ_2 D_{sd2} \frac{1}{T_2(yQ_2)}\right] + [(1-y)Q_2 + Q_1] \left[\frac{(1-y)Q_2 + Q_1}{\left(\frac{(1-y)Q_2}{D_{sd2}} + \frac{Q_1}{D_{sd1}}\right)}\right] \times \left[\frac{1}{T_{12}[(1-y)Q_2 + Q_1]}\right] \quad (3)$$

The advantage of the proposed 2D model is to be analytically tractable. On the face of it, it is not optimal because diffusive transport depends on the real 3D geometry of the porous structure which details are lost on any 2D representation. This limitation is considered in the model by attributing tortuosity coefficients to the diffusive phases or components. However, that implies a difficulty for determining these parameters. It is investigated in the paper whether the parameters of the proposed model can be estimated using established models and justified physical assumptions. As it will be shown in Section 2.4 when determining the model parameters for OPC pastes, total and percolating volumetric proportions of the diffusive phases can be determined independently using respectively the Jennings and Tennis multiphase hydration model [20,21] and micro-structural models such as CEMHYD3D [17]. Self-diffusion coefficients (for tritiated water) and tortuosity coefficients of the diffusive phases and components will also be estimated independently using well-known physical data, simple micro-structural models and inverse analysis (see Section 2.4).

2.3. Application to OPC pastes

In OPC pastes, the phases which contribute to the diffusive transport of dissolved species in pore water are the capillary porosity and the C–S–H (because of their intrinsic porosities) [16]. It is proposed here to distinguish two types of C–S–H according to the Jennings model [20,21]: the Low Density (LD) and the High Density (HD). Three diffusive phases have thus to be considered to apply the composite method to OPC pastes: capillary porosity, LD and HD C–S–H. The self-diffusion coefficient D_{sd} (for a given diffusing species) of capillary porosity is higher than the one of C–S–H phases, and because of their higher porosity, the self-diffusion coefficient of LD C–S–H is supposed to be greater than the one of HD C–S–H. Three diffusive rates are then expected to be observed in the various systems depending on which diffusive phase or mixed components are percolating in the system.

We now review the main configurations that the system previously defined may exhibit. Starting with low w/c, it is assumed that neither capillary porosity, neither LD C–S–H, nor the mixed component composed of these two phases are percolating in the system (percolation thresholds of diffusive phases and/or mixed components will be discussed in more details in the next section). These two diffusive phases are thus considered to be embedded in the HD C–S–H, the whole consisting of a percolating diffusive component in which the transport is essentially controlled by the HD C–S–H. This case is depicted in Fig. 3(a). For increasing w/c, it is assumed that the mixed component composed of capillary porosity and LD C–S–H will progressively percolate in the system (Fig. 3(b1)) until full percolation (Fig. 3(b2)). Finally, for higher values of w/c, capillary porosity is assumed to progressively percolate in the system (Fig. 3(c1)) until full percolation (Fig. 3(c2)).

As specified in the previous section, in the case when w/c is high, HD C–S–H are disposed in parallel in the assemblage although they will probably not percolate in such systems because of their low volume fractions. This assumption is justified by the fact that their contribution to diffusive transport is negligible in these cases, due precisely to these low volume fractions and their low diffusivity. On the contrary, for very low w/c (Fig. 3(a)), HD C–S–H are disposed in series in the systems although they do percolate. For these cases, the disposition in series for capillary porosity and LD C–S–H is equivalent to consider these phases as inclusions embedded in a matrix of HD C–S–H, this latter controlling the transport. It was checked that this last description is valid by calculating the effective diffusion coefficients of systems consisting of a diffusive matrix in which

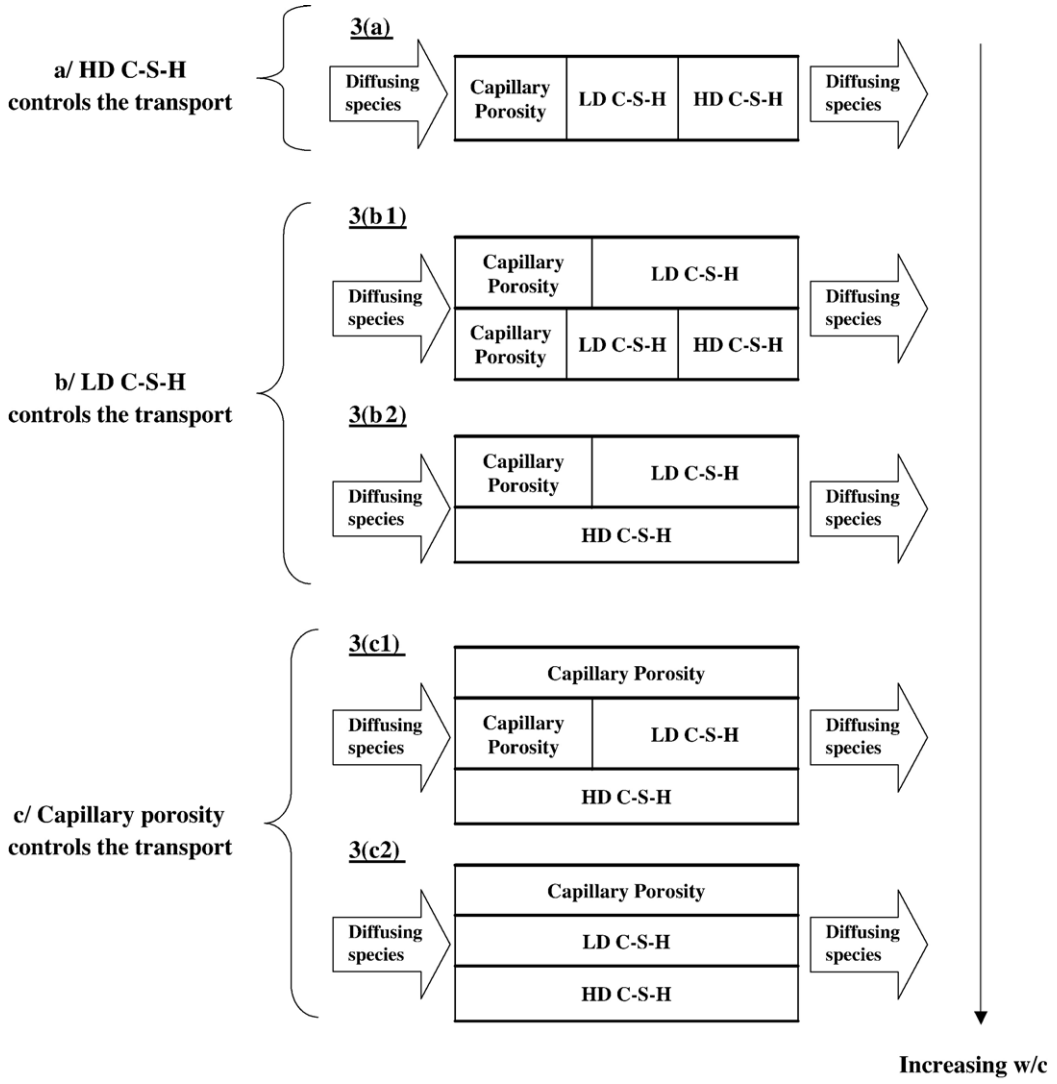

Fig. 3. Disposition of the diffusive phases of OPC pastes for increasing w/c in the Microtrans model.

are embedded small quantities of more diffusive spherical inclusions using several effective medium approximation schemes (Maxwell, Self-Consistent method, Differential Effective-Medium approximations) see e.g. [15] or a simple series model (without accounting for any tortuosity coefficient). For volume fractions of inclusions lower than 0.15 (this value corresponds to the percolation threshold of the diffusive phases or mixed components in OPC pastes in the model, see Section 2.4.2), results were close for the different methods.

The application of the model to OPC pastes finally leads to the equivalent systems presented in Fig. 3. The input parameters of the Microtrans model are the volume fractions of the diffusive phases. The intrinsic parameters of the model are the self-diffusion coefficients (for a given diffusing species) of the diffusive phases and the percolation functions and tortuosity coefficients of the various diffusive phases or mixed components. The non-diffusive inclusions (anhydrous, portlandite, AFm, Aft, etc.) are indirectly taken into account via the estimation of the tortuosity coefficients of the diffusive components, as it will be shown in Section 2.4.3.

The various parameters of the model are determined in the next section for OPC pastes. As stated before, the model will not be applied to the case of BFS-PFA cement pastes because no hydration model precise enough is available for this type of material.

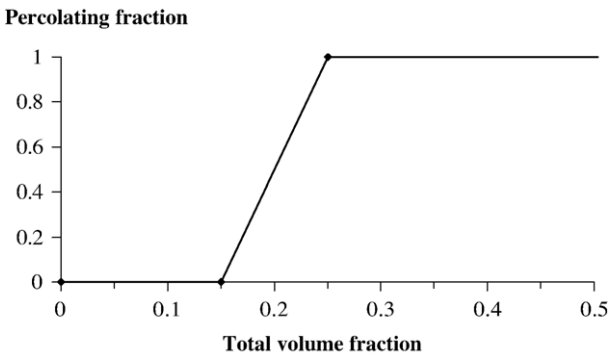

Fig. 4. Percolation function of the diffusive phases in the Microtrans model.

2.4. Determination of the model parameters

2.4.1. Mineralogical compositions

The mineralogical compositions of the studied OPC pastes (which HTO diffusion results are presented in Fig. 1) are determined using the Jennings and Tennis model [20,21], and given in Table 2. As the hydration degrees (α) of OPC pastes used for diffusion experiments were not precisely known, they were determined using Eq. (4) which links the w/c and the maximal hydration degree of OPC pastes cured under water. This equation was obtained by fitting a number of experimental results given in the literature [23,27–30].

$$\alpha = 0.239 + 0.745 \tanh[3.62(\mathrm{w/c} - 0.095)] \quad (4)$$

2.4.2. Percolation functions

The percolation function of capillary porosity in OPC pastes has been the topic of a number of studies (see e.g. [16,31–35]), but it still remains an open question for which no consensus has yet been reached. On the basis of 3D-hydration simulations performed with the CEMHYD3D code [16,30], the percolation threshold of capillary porosity was found to be situated somewhere between 15% and 20%. This result was confirmed by Differential Scanning Calorimetry studies of ice formation in the pore structure of hydrating OPC pastes [35]. 3D-hydration simulations performed with SPACE code found percolation threshold values of the same order (near 20%) [32]. However, simulations performed with IPKM (in the case of C_3S pastes) [33] and HYMOSTRUC [34] codes gave much lower percolation thresholds, in the range of a few percent. These variations are due to dissimilarities in the hydration principles and in the space discretization sizes of these various 3D codes.

The percolation function of the diffusive components used in the Microtrans model is shown in Fig. 4. It is supposed to be the same for the various diffusive components and it is inspired from 3D-hydration simulation performed with the CEMHYD3D code [16]. As other data exist in the literature, this point can possibly evolve in the future. However, this percolation function allows performing some interpretations about the diffusion results obtained experimentally for OPC pastes (see Fig. 1). The diffusion coefficients show a first important increase for the w/c equal to 0.30. This increase probably corresponds to the beginning of the percolation of the mixed component composed of capillary porosity and LD C–S–H (passage from Fig. 3(a) to (b1)). The volume fraction of this mixed component is equal to 19.1% (see Table 1). The use of the percolation function given in Fig. 4 induces that 7.8% of this mixed component would percolate in the system, what finally would correspond to 4.8% of LD C–S–H percolating in the system (through this mixed component). The diffusion coefficients present a second increase for the w/c equal to 0.45. As for it, this increase would correspond to the beginning of the percolation of capillary porosity that reaches 15.9% in this system according to Table 2 (passage from Fig. 3(b2) to (c1)).

2.4.3. Self-diffusion coefficients and tortuosity coefficients

This section is devoted to the estimation of the (tritiated water) self-diffusion coefficients and tortuosity coefficients of the diffusive phases in OPC pastes, on the basis of the macroscopic diffusion results presented in Fig. 1. It is attributed to the self-diffusion coefficient of capillary porosity the one of the considered diffusing specie (here tritiated water) in water: 2.24×10^{-9} m^2 s^{-1} at 25 °C [36,37]. Even if this value is only valid in the limit of infinite dilution, what is not the case for the pore water contained in capillary porosity, it is used here in the model in first approximation. The evolution of the tortuosity coefficient of capillary porosity (T_{CP}) as a function of its volume fraction is identified using the diffusion results obtained for the more porous pastes (w/c > 0.45) (see Fig. 1) so that experimental and modeling results are in good agreement. An exponential evolution, which has been successfully applied in another context [14], is chosen according to Eq. (5).

$$\frac{1}{T_{CP}(Q)} = 0.0067 \exp[5.0Q] \quad (5)$$

Both LD and HD C–S–H are supposed to be characterized by the same tortuosity coefficient ($T_{LD\ CSH} = T_{HD\ CSH}$), as explained below. The evolution of their tortuosity coefficient as a function of their volume fraction has been estimated by means of the well-known two phase composite sphere model of Hashin (see e.g. [15]). This model allows in particular calculating the tortuosity coefficient of a percolating solid matrix in which the concentration of non-diffusive spherical inclusions is progressively increased. It is assumed that, as soon as they are percolating in

Table 2
Hydration degrees (%) and mineralogical compositions (volume %) of OPC pastes determined using the Jennings and Tennis model

w/c	Hydration degree	Capillary porosity	LD C–S–H	HD C–S–H	$Ca(OH)_2$	AFt–AFm C_4AH_{13}	$C_3(A,F)H_6$	Anhydrate
0.25	62.1	4.6	8.7	38.4	14.3	7.2	7.3	19.5
0.30	70.8	7.1	12.0	37.4	15.2	7.4	7.2	13.7
0.35	78.2	9.7	16.8	33.9	15.6	7.5	7.2	9.4
0.38	81.7	11.5	20.2	30.7	15.6	7.3	7.3	7.5
0.40	83.8	12.7	22.6	28.3	15.5	7.2	7.3	6.4
0.42	85.6	14.0	25.1	25.7	15.4	7.1	7.3	5.4
0.45	87.9	15.9	28.8	21.6	15.1	6.9	7.3	4.3
0.50	90.8	19.2	34.8	14.6	14.4	6.5	7.5	3.0
0.60	94.6	25.0	47.0	1.0	13.1	5.8	6.8	1.4
0.65	95.8	27.7	47.0	0.0	12.5	5.5	6.4	1.0

the system, both LD and HD C–S–H can effectively be seen as forming continuous solid matrixes. This last point has already been considered elsewhere for the whole C–S–H phase [38]. It should be noticed that the coated sphere model of Hashin, which provides exact results whatever the volume fractions of the phases may be extended according to the reasoning given in [39] to conform with the idea of the potential simultaneous percolation for the two phases (LD and HD C–S–H). Indeed, Gilormini has shown that the same exact value of effective diffusivity can be obtained by mixing two types of coated spheres, the second type differing from the first by phase inversion between the core and the coating. These two coated spheres, when assembled according to the Hashin model, define the upper and lower Hashin–Shtrikman bounds for the prescribed effective diffusivity. The mix is then possible precisely because the two coated sphere types have the same effective diffusivity in the sense of the Hashin model, and consequently one type sphere can be replaced by the other without perturbing the overall system. Since the Hashin model implies that the size distribution of the spheres ranges to the infinitesimally small, it is expected that the two phases would percolate with an appropriate mix of the two types of spheres.

It has been explained before that mixed components have also to be considered in the calculations (capillary porosity + LD C–S–H + HD C–S–H and/or capillary porosity + LD C–S–H) (see 2.2, 2.3 and Fig. 3). It is assumed that the tortuosity coefficient of these mixed components is the same as the one determined for LD and HD C–S–H alone. It would mean that as soon as they are percolating, these mixed components can *geometrically* be seen as forming matrixes.

The HTO self-diffusion coefficients of LD and HD C–S–H remain the only unknown parameters at this stage. They are adjusted using the macroscopic results presented in Fig. 1. The HTO self-diffusion coefficient of HD C–S–H is identified using principally the experimental diffusion results obtained for the lowest w/c (0.25 and 0.30), although diffusion results related to medium w/c values (0.35 to 0.42) were used for LD C–S–H diffusivity identification. The HTO self-diffusion coefficients were found to be equal to 9×10^{-12} and 1×10^{-12} m^2 s^{-1} respectively for LD and HD C–S–H.

All the results are synthesized in Fig. 5 in which the HTO effective diffusivities of the various elementary phases are expressed as a function of their volume fractions. HTO diffusivities of mixed components are not represented in Fig. 5. They

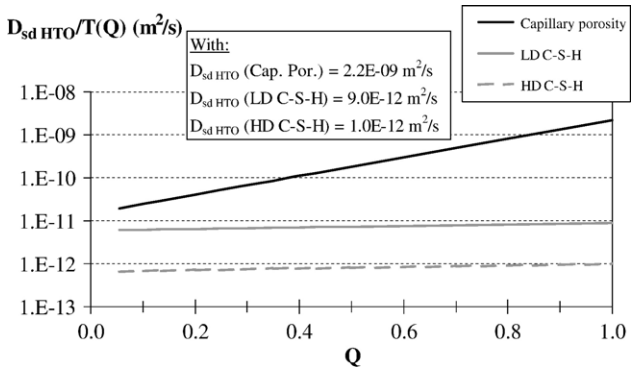

Fig. 5. HTO effective diffusivities ($D_{sd}/T(Q)$) of the OPC paste diffusive phases.

can be simply calculated using the parameters determined above depending on the composition of these mixed components. Fig. 5 shows that capillary porosity has a higher tortuosity coefficient compared to the one of HD and LD C–S–H. An explanation may be for example that capillary porosity contains a lot of dead-end pores. Using the parameters determined in this section, the simplified composite model allows calculating De_{HTO} for each studied OPC paste with less than 15% error, as shown in Fig. 1. It is worth noting that the model can be extended to other diffusing species by using Eq. (6), based on the formulation proposed in Ref. [40]. It has to be mentioned however that care must be taken when predicting an effective diffusion coefficient using Eq. (6) because of the impact of speciation and, more precisely, the impact of electro-diffusion on diffusive transport [41].

$$De_{DS} = De_{HTO}\cdot\frac{D_{sd\ DS}}{D_{sd\ HTO}} \tag{6}$$

where De_{DS} is the effective diffusion coefficient of the considered diffusing species (DS) in the material, $D_{sd_{DS}}$ and $D_{sd_{HTO}}$ are respectively the self-diffusion coefficients of the considered diffusing species and of HTO in the pore solution.

3. Application of the simplified composite model to the determination of porosity–diffusion evolutions

As the intrinsic parameters of the Microtrans model have been determined, it can be used to estimate the effective diffusivity of cement pastes submitted to porosity opening or plugging. For porosity opening, the scenario considered is a leaching inducing a progressive dissolution of portlandite, calcium aluminate phases and anhydrous (the C–S–H decalcification is not supposed to create additional porosity in the system [14]). This sequence corresponds to the description adopted to model the leaching of OPC pastes using a coupled chemo-transport model (see Section 4). The leaching of the hydrates of OPC pastes is taken into account in the Microtrans model by progressively increasing the volume fraction of capillary porosity in the system. For the filling-in of porosity, in this application the capillary porosity is supposed to plug first, leading to a decreasing of its volume fraction till zero. A limitation of the model must be specified at this stage. Modeling studies performed using the CEMHYD3D code have shown that hydration and leaching can probably not be considered as being simply inverse processes regarding capillary porosity percolation phenomena [42]. Re-percolation of capillary porosity seems to occur at a smaller value than that at which the initial de-percolation during hydration occurred (e.g. respectively 0.16 versus 0.18 for a 0.45 w/c OPC paste). In first approximation, this effect is not taken into account into the composite model. Moreover, as degradation consists of dissolving and/or precipitating different mineral phases, the tortuosity coefficient of capillary porosity is probably not a single-valued function of its volume fraction, but is more likely path-dependant. In first approximation, the tortuosity

coefficient of capillary porosity determined on the basis of experimental results related to sound OPC pastes with various porosities (see Section 2.4.3) will be used here to describe opening and plugging of capillary porosity in OPC pastes.

Concerning C–S–H porosity plugging, HD and LD C–S–H porosities are supposed to plug simultaneously. As shown in Fig. 6, the filling-in of the C–S–H porosity is taken into account by decreasing their HTO self-diffusion coefficients according to a simple Archie law. Porosities of sound LD and HD C–S–H are defined as being equals to 20% and 31% in reference to the Jennings model [43], and excluding pores smaller than 1 nm. The water in these small pores probably contributes negligibly to the overall transport because it is strongly fixed on the solid surfaces [23]. These C–S–H porosity values are also supported by the fact that total porosities of the studied cement pastes calculated using the Jennings and Tennis model by summing capillary porosity and C–S–H porosities are in very good agreement with total water porosities measured next to a 60 °C oven-drying on OPC pastes made with the same cement and various water to cement ratios [24].

Fig. 7 presents the porosity–diffusion evolutions obtained from the Microtrans model for three OPC pastes with various w/c in order to study materials over a wide range of performances. It indicates an important evolution of the effective diffusion coefficient for the 0.50 w/c paste with the initial opening of porosity. This effect is related to the progressive percolation of capillary porosity. When all the capillary porosity percolates, the evolution becomes less important. For the 0.40 w/c paste, the first porosity opening percentages induce only a low augmentation of the diffusivity. Then, for further porosity opening, capillary porosity starts percolating in the system and a behavior comparable to the one of the 0.50 w/c paste is observed. For the 0.25 w/c paste, an important evolution of the diffusion coefficient can be observed over a large range of porosity opening. This is due to the fact that, first, the percolating fraction of the mixed component including LD C–S–H and capillary porosity increases in the system (passage from the system described in Fig. 3(b1) to the one described in Fig. 3(b2)). Second, capillary porosity itself starts percolating gradually in the system. To summarize, the diffusive flow of the 0.25 w/c OPC paste is initially controlled by HD C–S–H; when submitted to leaching, the diffusivity becomes progressively controlled by LD C–S–H and then by capillary porosity. Finally, it appears that for total porosity greater than about 0.25, the diffusivity evolutions are very similar for the different materials.

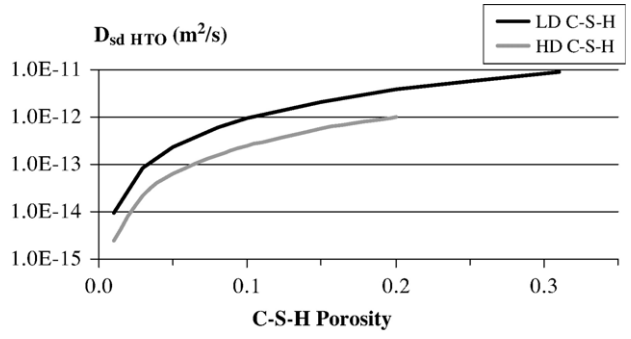

Fig. 6. HTO self-diffusion coefficients of LD and HD C–S–H as a function of plugging of their porosity according to a simple Archie Law.

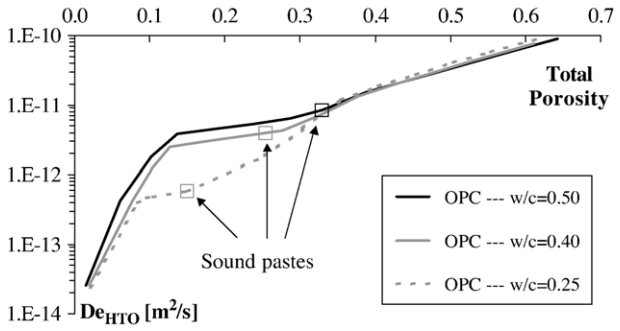

Fig. 7. Porosity–diffusion evolutions (HTO) determined for various OPC pastes using the simplified composite model.

Concerning the filling-in of porosity, the initial plugging of capillary porosity only decreases a little the diffusion coefficients in the cases of the 0.25 and 0.40 w/c pastes because this phase does not control the transport in the corresponding sound systems (see Fig. 7). Then, the filling-in of C–S–H porosity induces significant reductions in the effective diffusion coefficients of these pastes. It is emphasized that other scenario could be envisaged on the basis of this model depending on the degradation phenomenon (carbonation, sulfate attack...), as for example a concomitant plugging of capillary porosity and C–S–H. For the 0.50 w/c paste, the first few percentages of initial filling of capillary porosity lead to a significant decrease of the diffusivity, because they induce a complete de-percolation of this phase in the system. The phenomena related to the subsequent porosity decreasing are the same than those described for the 0.25 and 0.40 w/c pastes.

It has been shown in this section that the simplified composite model is useful to determine the diffusivity evolutions of OPC pastes submitted to porosity changes. Because the corresponding calculations are performed easily, the model can thus be simply implemented into coupled numerical chemo-transport models aiming at describing for example the leaching of cementitious materials, as described in the next section.

4. Implementation of the Microtrans model into a simplified chemo-transport model describing the leaching of cementitious materials

4.1. Presentation of the coupled chemo-transport model (Diffu-Ca)

The numerical tool Diffu-Ca used for the simulation of cementitious material leaching by pure water has already been presented elsewhere in details [14,44]. Leaching of hydrated cement is due to dissolved chemical species concentration gradients between the interstitial solution and the leachant, generating diffusion of these species through the material pore solution. The chemical equilibria of the system are thus modified. These chemical modifications are in turn at the origin of the progressive portlandite and aluminate hydrates (AFm, AFt, etc.) dissolution and the C–S–H decalcification. The numerical

model is based on the generalized transport equation of calcium. A single variable, namely the calcium concentration in the pore solution C_{ca}, allows to fully describe the problem. Indeed, the dissolution of portlandite and aluminates hydrates, and the decalcification of C–S–H can both be computed as a function of this single variable. Chemical equilibria are thus taken into account using the equilibrium curve between the calcium concentration in the solution and in the main solid phases (C–S–H, portlandite, AFm, Aft, etc.). The evolution of C_{ca} is modeled using Eq. (7).

$$\frac{\partial(\Phi C_{ca})}{\partial t} = \mathrm{div}[D_e grad(C_{ca})] - \frac{\partial S_{ca}}{\partial t} \quad (7)$$

where Φ, C_{ca}, t, D_e, S_{ca} are respectively the porosity, the calcium concentration in the pore solution, the time, the effective diffusion coefficient and the content of calcium in soluble solid phases per unit volume of porous material. Eq. (7) is solved numerically using a mixed-hybrid finite element formulation in the Cast3m code developed at CEA [45].

4.2. Application, results and discussion

In order to test them, the porosity–diffusion evolutions as determined for various OPC pastes in Section 3 are implemented into the Diffu-Ca model to perform leaching calculations under pure water. It was shown elsewhere that using HTO porosity–diffusion evolutions was an acceptable approximation to solve Eq. (7) [6,14]. It is reminded that the porosity–diffusion equation issued from the CEMHYD3D code [16] has also been successfully implemented into a model simulating OPC paste leaching [46]. A limitation of these simulations is that only portlandite dissolution was modeled.

Fig. 8 presents the equilibrium curves between the calcium concentration in the pore solution C_{ca} and the content of calcium in soluble solid (per unit volume of porous material) S_{ca} for the three studied pastes, on the basis of the following assumptions [14]:

– the alkalis are not taken into account in the chemical equilibria (the modeling results will be compared to leaching experiments performed on pastes in which alkalis were already leached up during their curing in lime–water),
– portlandite linearly dissolves when C_{ca} decreases from 22 to 21 mmol/l,
– Ca/Si ratio of C–S–H linearly decreases from 1.7 to 1.0 and aluminate phases dissolve when C_{ca} decreases from 21 to 2 mmol/l,
– Ca/Si ratio of C–S–H linearly decreases from 1.0 to 0.5 and anhydrous phases dissolve (unless C_4AF as it was shown in Ref. [47]) when C_{ca} decreases from 2 to 1.5 mmol/l,
– Ca/Si ratio of C–S–H linearly decreases from 0.5 to 0 when C_{ca} decreases from 1.5 to 0 mmol/l.

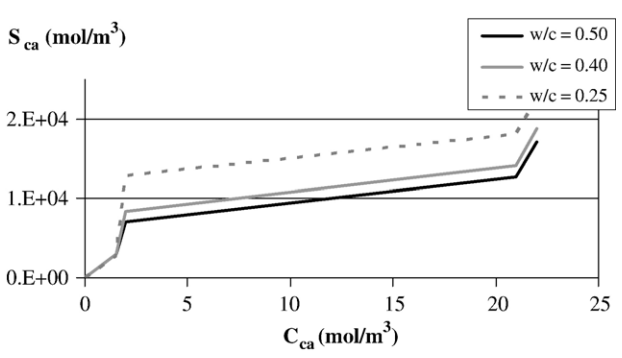

Fig. 8. Equilibrium between the calcium concentration in the pore solution (C_{ca}) and in the main solid phases (S_{ca}) for OPC pastes (w/c equals to 0.50, 0.40 and 0.25).

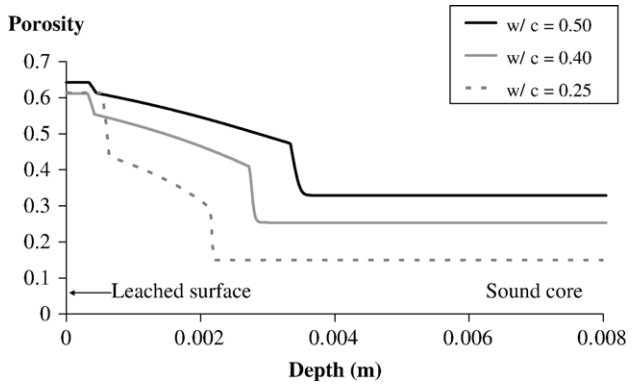

Fig. 9. Simulated total porosity profiles of OPC pastes after 400 day leaching under pure water.

Figs. 9 and 10 respectively present total porosity and effective diffusion coefficient profiles obtained from Diffu-Ca simulations for the studied OPC pastes submitted to 400 day leaching under pure water. Table 3 synthesizes the results obtained for the three pastes in terms of leaching rate (R_L) and ratio between the effective diffusivity of the leached zone and the one of the sound material (R_D). Table 3 also integrates experimental data measured in quite similar conditions to that of modeling when they are available (leaching under pure water of OPC pastes having the same w/c and from which the alkalis were leached up during curing). The leached zone is defined as the one which does not

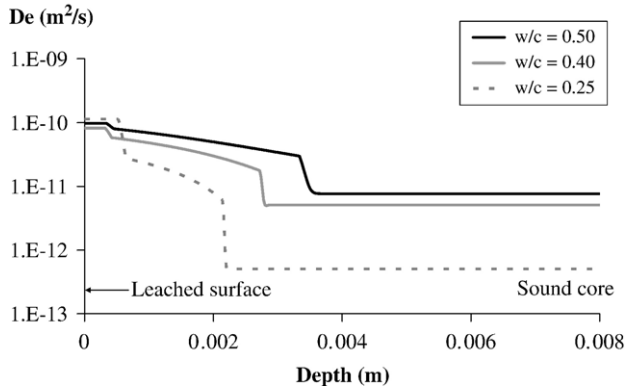

Fig. 10. Simulated effective diffusivity profiles of OPC pastes after 400 day leaching under pure water.

Table 3
Results of leaching simulations using the Diffu-Ca code for OPC pastes (R_D and R_L) and comparison to experimental data

w/c	Modeling results		Experimental data	
	R_L (Leaching rate (10^{-7} m $s^{-0.5}$))	R_D (ratio between diffusivities of leached and sound zone)	R_L	R_D
0.50	5.95	6.1	–	–
0.40	4.80	6.3	4.76 [6]	7 [48]
0.25	3.64	27.5	2.52 [49]	–

contain any more portlandite. Effective diffusion coefficient of this heterogeneous zone (De_{eq}) is calculated according to Eq. (8).

$$De_{eq} = \frac{x_L}{\int_0^{x_L} \frac{dx}{De(x)}} \quad (8)$$

where x_L is the depth of the leached zone.

Numerical results indicate that leaching rates decrease respectively from 5.95×10^{-7} to 3.64×10^{-7} m $s^{-0.5}$ when the w/c decreases from 0.50 to 0.25. On the contrary, in the meantime R_D ratios increase from 6.1 to 27.5. The low diffusivity of the sound paste at low w/c induces a low rate of evacuation of calcium coming from the initial dissolution of portlandite. Furthermore, taking into account the assumption of anhydrous dissolution used in the calculations, the porosity and the diffusivity of the completely leached low w/c paste are comparable to the ones of the completely leached higher w/c pastes. Considering this point and the lowest diffusivity of the sound low w/c paste explains the higher R_D ratio for the low w/c paste.

Numerical results (R_L and R_D) are in good agreement with experimental data for the 0.40 w/c paste. For the 0.50 w/c paste, complementary experiments would be necessary to check the tendency given by the simulations. Lastly, in the case of the 0.25 w/c paste, simulations indicate a leaching rate 25% greater than the available experimental value. However, it is recalled that the cement paste used for the experimentation was cast using a different cement from the one used in this study. This variation in the composition of the initial system may have an impact on the leaching rate R_L (as it might also be the case when comparing modeling and experimental R_L for the 0.40 w/c paste). Another explanation could be situated in the fact that for low w/c paste, a fraction of the anhydrous phases (in particular C_3S because of its high reactivity) would be completely surrounded by a shell of C–S–H. During leaching, these anhydrous could dissolve through this shell leading to:

- an increase of the non-connected fraction of capillary porosity instead of the connected one, thus generating a weaker increase in the diffusivity of the leached zone compared to the current one,
- an additional kinetics for the dissolution of these anhydrous through C–S–H shells, and thus an additional delay for the leach rate.

Further experimental investigations would be necessary to check these assumptions. For example, scanning electron microscopy characterization of the leached zone of a low w/c paste could give some answers to these questions.

To summarize, the simplified composite model thus makes it possible to correctly simulate the effects of local chemistry changes on local diffusivity evolutions in the case of the decalcification of 0.40 and 0.50 OPC pastes. Further developments would be necessary to improve the treatment of low w/c pastes.

5. Conclusion

A simplified composite model, namely Microtrans, has been presented in this paper. It aims at linking the main features of the microstructure and the effective diffusion coefficient of dissolved chemical species diffusing in saturated OPC pastes. The method considers the system at the scale of the mineralogical assemblage. Its purpose is to estimate the equivalent diffusivity of the whole system by accounting for the self-diffusion coefficients (for a given species) of the various components of the microstructure and the way in which the latter are arranged in the space. This simplified approach makes it possible to be freed from a multi-scale characterization of the porosity, which it is not possible to reach completely today using the available experimental techniques. In this framework, the diffusive phases of the microstructure are supposed to be the capillary porosity and the Low Density and High Density C–S–H. The self-diffusion coefficient of capillary porosity is higher than the one of C–S–H whereas, because of their higher porosity, the self-diffusion coefficient of LD C–S–H is supposed to be higher than the one of HD C–S–H. For OPC pastes, the diffusive transport should thus be essentially controlled by the most diffusive phase percolating in the system. In the model, various parameters account for the microstructural properties of the diffusive phases (related to their overall 3D-disposition in the microstructure) that have a critical impact on the diffusivity of the whole system (volume fractions, percolation properties and tortuosity coefficients). The HTO self-diffusion coefficients and the microstructural parameters are assessed for the diffusive phases of OPC pastes in this paper. The model is thus available to estimate the local evolutions of the effective diffusion coefficient according to porosity opening or plugging due to dissolution or precipitation of minerals in the system when it is submitted for example to underground water solicitations. This simple model based on a phenomenological description of the processes, and with well-defined physical parameters, can be easily implemented into coupled chemo-transport numerical models.

The porosity–diffusion evolutions calculated from the composite model for three OPC pastes were implemented into a simplified chemo-transport model aiming at describing the leaching of cementitious materials under pure water. Leaching simulations showed good agreement with the available experimental data for the 0.40 w/c paste. Further leaching experiments would be necessary to allow a complete comparison between numerical and experimental results for the 0.50 and 0.25 w/c pastes.

Most of the parameters of the Microtrans model were identified, or determined on the basis of simulations performed with

various models found in the literature. Further experimental developments would be necessary in order to directly measure or identify the parameters taken into account in the model. In addition, due to its flexible formalism, the model could be simply extended to the case of blended BFS-PFA cement pastes. However, the knowledge of the mineralogical composition of this type of materials, in particular in term of different types of C–S–H, is still insufficient to consider this application immediately.

The proposed method could also be applied to up-scale diffusive properties from the scale of cement paste, aggregates and Interfacial Transition Zones to the one of concrete. However, it would probably not bring significant progress in comparison with efficient existing models already available to achieve this goal (see e.g. [7–11]).

Acknowledgments

The authors would like to thank ANDRA and COGEMA (AREVA) for financial support.

References

[1] A.W. Harris, A. Atkinson, V. Balek, K. Brodersen, G.B. Cole, A. Haworth, Z. Malek, A.K. Nickerson, K. Nilsson, A.C. Smith, The performance of cementitious barriers in repositories, European Commission Nuclear Science and Technology Report, Report EUR 17643 EN, 1998.
[2] H. Peycelon, F. Adenot, P. Le Bescop, C. Richet, V. Blanc, Long-term behavior of concrete: development of operational model to predict the evolution of its containment performance, application to cemented waste packages, Int. Conf. Global 2001, International conference on “Back-End of the Fuel Cycle: From Research to Solutions”, vol. 1, 2001, Abstract 131, Paris, France.
[3] S. Kamali, Comportement et simulation des matériaux cimentaires en environnements agressifs: lixiviation et température, PhD thesis, Ecole Normale Supérieure de Cachan, France, 2003.
[4] B. Bary, P. Le Bescop, Simplified chemo-transport Modeling of carbonation and sulphate attack in saturated cement pastes, Int. Conf. Computational mechanics WCCM VI in conjunction with APCOM’04, Tsinghua University Press and Springer-Verlag, Vol II, no. 408, Beijing, China, 2004.
[5] Y. Maltais, E. Samson, J. Marchand, Predicting the durability of Portland cement systems in aggressive environments—laboratory validation, Cem. Concr. Res. 34 (2004) 1579–1589.
[6] C. Tognazzi, Couplage Fissuration—Dégradation Chimique dans les Matériaux cimentaires: Caractérisation et Modélisation, PhD Thesis, INSA Toulouse, France, 1998.
[7] D.P. Bentz, R.J. Detwiler, E.J. Garboczi, P. Halamickova, M. Schwartz, Multi-scale modeling of the diffusivity of mortar and concrete, in: L.O. Nilsson, J.P. Ollivier (Eds.), Chloride Penetration into Concrete, RILEM, 1997, pp. 85–94.
[8] D.P. Bentz, Influence of silica fume on diffusivity in cement based materials, II. Multi-Scale Modeling of Concrete Diffusivity, Cem. Concr. Res. 30 (2000) 1121–1129.
[9] E.J. Garboczi, L.M. Schwartz, D.P. Bentz, Modeling the influence of the interfacial zone on the DC electrical conductivity of mortar, Adv. Cem. Based Mater. 2 (1995) 169–181.
[10] E.J. Garboczi, D.P. Bentz, Multiscale analytical/numerical theory of the diffusivity of concrete, Adv. Cem. Based Mater. 8 (1998) 77–88.
[11] E.J. Garboczi, J.G. Berryman, New effective medium theory for the diffusivity or conductivity of a multi-scale concrete microstructure model, Concr. Sci. Eng. 2 (2000) 88–96.
[12] O. Truc, J.P. Ollivier, L.O. Nilsson, Numerical simulation of multi-species diffusion, Mater. Struct. Chem. Biol. Phys. Technol. 33 (2000) 566–573.
[13] P. Tumidajski, A.S. Schumacher, S. Perron, P. Gu, J.J. Beaudoin, On the relationship between porosity and electrical resistivity in cementitious systems, Cem. Concr. Res. 26 (1996) 539–544.
[14] M. Mainguy, C. Tognazzi, J.M. Torrenti, F. Adenot, Modeling of leaching in pure cement paste and mortar, Cem. Concr. Res. 30 (2000) 83–90.
[15] S. Torquato, Random Heterogeneous Media: Microstructure and Macroscopic Properties, Springer-Verlag, New York, 2001.
[16] D.P. Bentz, O.M. Jensen, A.M. Coats, F.P. Glasser, Influence of silica fume on diffusivity in cement based materials, I. Experimental and computer Modeling studies on cement pastes, Cem. Concr. Res. 30 (2000) 953–962.
[17] D.P. Bentz, Three dimensional computer simulation of cement hydration and microstructure development, J. Am. Ceram. Soc. 80 (1997) 3–31.
[18] E.J. Garboczi, D.P. Bentz, Computer simulation of the diffusivity of cement-based materials, J. Mater. Sci. 27 (1992) 2083–2092.
[19] B.H. Oh, S.Y. Jang, Prediction of diffusivity of concrete based on simple analytic equations, Cem. Concr. Res. 34 (2004) 463–480.
[20] H.M. Jennings, A model for the microstructure of calcium silicate hydrate in cement paste, Cem. Concr. Res. 30 (2000) 101–116.
[21] P. Tennis, H.M. Jennings, A model for two types of calcium silicate hydrate in the microstructure of Portland cement pastes, Cem. Concr. Res. 30 (2000) 855–863.
[22] B. Bary, S. Bejaoui, Assessment of diffusive and mechanical properties of hardened cement pastes using a multi-coated sphere assemblage model, Cem. Concr. Res. 36 (2006) 245–258.
[23] V. Baroghel-Bouny, Caractérisation des pâtes de ciment et des bétons, LCPC, Paris, France, 1994.
[24] C. Gallé, Effect of drying on cement-based materials pore structure as identified by mercury intrusion porosimetry: a comparative study between oven-, vacuum-, and freeze-drying, Cem. Concr. Res. 31 (2001) 1467–1477.
[25] L.M. Schwartz, N. Martys, D.P. Bentz, E.J. Garboczi, S. Torquato, Cross-property relations and permeability estimation in model porous media, Phys. Rev., E Stat. Phys. Plasmas Fluids Relat. Interdiscip. Topics 48 (1993) 4584–4591.
[26] J.G. Berryman, Bounds and estimates for transport coefficients of random and porous media with high contrasts, J. Appl. Phys. 97 (2005) 063504.
[27] N.J. Carino, K.W. Meeks, Curing of High-Performance Concrete: Phase I study, National Institute of Standards and Technology Report, NISTIR 6505, 2001.
[28] S. Igarashi, M. Kawamura, A. Watanabe, Analysis of cement pastes and mortars by a combination of backscatter-based SEM image analysis and calculations based on the Powers model, Cem. Concr. Compos. 26 (2004) 977–985.
[29] L. Lam, Y.L. Wong, C.S. Poon, Degree of hydration and gel/space ratio of high-volume fly ash/cement systems, Cem. Concr. Res. 30 (2000) 747–756.
[30] I. Pane, W. Hansen, Investigation of blended cement hydration by isothermal calorimetry and thermal analysis, Cem. Concr. Res. 35 (2005) 1155–1164.
[31] E.J. Garboczi, D.P. Bentz, The effect of statistical fluctuation, finite size error, and digital resolution on the phase percolation and transport properties of the NIST cement hydration model, Cem. Concr. Res. 31 (2001) 1501–1514.
[32] J. Hu, P. Stroeven, Depercolation threshold of porosity in model cement: approach by morphological evolution during hydration, Cem. Concr. Compos. 27 (2005) 19–25.
[33] P. Navi, C. Pignat, Three-dimensional characterization of the pore structure of a simulated cement paste, Cem. Concr. Res. 29 (1999) 507–514.
[34] G. Ye, Percolation of capillary pores in hardening cement pastes, Cem. Concr. Res. 35 (2005) 167–176.
[35] K.A. Snyder, D.P. Bentz, Suspended hydration and loss of freezable water in cement pastes exposed to 90% relative humidity, Cem. Concr. Res. 34 (2004) 2045–2056.
[36] R. Mills, V.M.M. Lobo, Self-Diffusion in Electrolyte Solutions, Elsevier, Amsterdam, 1989.
[37] C. Richet, Etude de la migration des radioéléments dans les liants hydrauliques—Influence du vieillissement des liants sur les mécanismes et la cinétique des transferts, PhD Thesis, Paris XI Orsay, France, 1992.
[38] D.P. Bentz, E.J. Garboczi, N.S. Martys, Application of digital-image-based models to microstructure, transport properties, and degradation of cement-

based materials, in: H.M. Jennings, J. Kropp, K. Scrivener (Eds.), The Modelling of Microstructure and Its Potential for Studying Transport Properties and Durability, Kluwer, Dordrecht, 1996, pp. 167–185.
[39] P. Gilormini, Realizable compressibility and conductivity in isotropic two-phases composites, C. R. Acad. Sci. Paris t. 329 (2001) 851–855 (Série II b).
[40] K.A. Snyder, The relationship between the formation factor and the diffusion coefficient of porous materials saturated with concentrated electrolytes: Theoretical and experimental considerations, Concr. Sci. Eng. 3 (2001) 216–224.
[41] K.A. Snyder, J. Marchand, Effect of speciation on the apparent diffusion coefficient in non-reactive porous systems, Cem. Concr. Res. 31 (2001) 1837–1845.
[42] D.P. Bentz, E.G. Garboczi, Modeling the leaching of calcium hydroxide from cement paste: effects on pore space percolation and diffusivity, Mater. Struct. Chem. Biol. Phys. Technol. 25 (1992) 523–533.
[43] H.M. Jennings, Colloid model of C–S–H and implications to the problem of creep and shrinkage, Mater. Struct. Chem. Biol. Phys. Technol. 37 (2004) 59–70.
[44] F. Adenot, A. Aspart, Modélisation de l'influence du débit de renouvellement de la solution agressive sur la cinétique de dégradation d'une pâte de ciment, Actes des 1ères Rencontres internationales "Sciences des Matériaux et Propriétés des Bétons", Toulouse, France, 1998.
[45] F. Dabbene, Mixed-hybrid finite elements for transport of pollutants by underground water, Proc. of the 10th Int. Conf. on Finite Elements in Fluids, Tucson, USA, 1998.
[46] J. Marchand, D.P. Bentz, E. Samson, Y. Maltais, Influence of calcium hydroxide dissolution on the transport properties of hydrated cement systems, Published in "Reactions of Calcium Hydroxide in Concrete", American Ceramic Society, Westerville, OH, 2001.
[47] V. Matte, Durabilité des bétons à ultra hautes performances: Rôle de la matrice cimentaire, PhD Thesis, Ecole Normale Supérieure de Cachan (France), Université de Sherbrooke (Canada), 1999.
[48] H. Lamotte, S. Béjaoui, Transport diffusionnel des matériaux cimentaires—synthèse des données, CEA Internal Report, CEA NT-SEEC-2004-06, 2004.
[49] A. Delagrave, J. Marchand, M. Pigeon, Durability of high performance cement pastes in contact with chloride solutions, 4th International Symposium on Utilization of High-strength/High-Performance Concrete. Paris, France, 1996.